Journal of Mathematical Control Science & Applications, Vol. 8 No. 2 (July-December, 2022)
ISSN : 0974-0570

A NOVEL APPROACH FOR DENOISING IMAGES BASED ON DIFFUSION EQUATION USING WAVELETS

AKMAL RAZA[1], ARSHAD KHAN[1] AND KHALIL AHMAD[2]

ABSTRACT. The main objective of this study is to develop a new algorithm based on diffusion equation using wavelets. We solved the diffusion equation by using finite difference method by taking noisy image as initial guess. After that we applied wavelet denoising scheme based on soft thresholding on the image which we obtain as a solution of diffusion equation. The idea behind this study is that, the linear diffusion equation is not capable to capture the edges during denoising process, so the edges are restored by using wavelets denoising process. To validate the developed scheme we compared peak signal to noise ratio (PSNR) with wavelet method, diffusion equation method and wavelet coefficients via diffusion equation method.

1. Introduction

Images are very powerful and widely used medium of communication and it is an easy way to present our physical world. A digital image comes from continuous world. It is obtained from an analogue image by sampling and quantization. The process depends upon quantization devices, for instance on compact disk for digital camera. The applications of images are very helpful in the field of computer science, for example robotics, video games, data compression, scanners and data transmission, etc. Also, images are very important in geophysics and geographical point of view such as oil exploration, nuclear test monitoring, earthquake measurement and remote sensing, aerial photography for detection of crop damage or forest fires, deep space probes and weather forecasting. Images are very useful in the field of medical science. In medical science many devices exist which produce images such as ultra-sounds and X-rays. Medical imaging has made substantial use of images from the earliest days. More interestingly, images are also useful in television transmission from lunar, video surveillance, road traffic analysis, water supplies, pollution, urbanization, etc. Image processing provides tools to track and quantify changes in above mentioned areas. A typical camera can give an image of size 320×320 to 3060×2036. In general, for digital camera we consider images of size 720×576 as standard format, 1920×1440 as high definition (HD) and 128×128 for medical imaging. Clearly higher the resolution, closer the digital image to physical world obtained. An image is a compactly supported real valued function in $L^2(\mathbb{R}^2)$ ([15], [22]).

It is well known to scientists and engineers with real world data that signal do not exist without noises, there are many cases when images corrupted. Images get corrupted during capture, transmission or imperfection of image acquisition. Natural noise degrades

2000 *Mathematics Subject Classification.* 65L12; 65N06; 65T60; 68U10.
Key words and phrases. Diffusion equation; Finite Difference; Image denoising; Wavelet Transform.

the quality of images. The challenge is to denoise or restore the image so that it can be clearly visible by human eye. Image processing and computer vision bring to mathematics a host of very challenging new problems and fascinating applications. Methods based on functional analysis, probability theory, statistics, wavelet analysis, linear and nonlinear filtering and partial differential equations are very useful in image processing, such as how to restore a degraded image or denoise and how to segment it into meaningful regions. Methods based on partial differential equations have been presented by many researchers such as, piecewise smooth image model by C Liu et al.[5], variable coefficient linear filter minimizing strictly convex non-quadratic functionals by Schnorr [7], method for total variation by Chang and Chern [34], nonlinear primal dual method by Chan et al [36], denoising with higher order derivatives by Scherzer [32], PDE based de-convolution by Welk [27], wavelet coefficient via Diffusion equation by Kumar et al [38], etc. Methods based on wavelets have been proposed by many researchers such as iterative shrinkage thresholding algorithm by A. Beck and M teboulle [1], single and multiband image denoising algorithm by A. Pizurrica and Philips[2], interscale and intrascale method by F Yan et al [14], Adaptive wavelet thresholding by Chang et al [35] and local contrast and adaptive mean in wavelet transform domain by Sharma et al [33]. Advanced algorithm based on wavelet have been discussed by Donoho ([10], [11]) , Donoho and Johnstone ([12], [13]),Johnstone and Silverman [18], Birge and Massart [23].

In this paper, we described diffusion equation and its existence and uniqueness of solution in section 2. In section 3, we described wavelet, wavelet transform, discrete wavelet transform, two dimensional discrete wavelet transform, and thresholding. In section 4, we proposed the method based on diffusion equation and wavelet. In section 5, we demonstrate four examples to show the superiority of our method and compared PSNR values with diffusion equation method, wavelet method and method presented by Kumar et al [38]. The conclusion is given in section 6.

2. Diffusion Equation

Partial differential equations (PDE) encounter in physics, biology, mechanics, finance and now in images. The theory of PDE is well established and belong to the mathematical analysis and very closely related to physical world. The oldest and most popular equation in image processing is heat equation, i.e., parabolic partial differential equation. Scientists and researchers pointed out that one parameter family of derived image can be equivalently viewed as the solution of the diffusion equation.
We consider the following linear diffusion equation:

$$\frac{\partial u(t,x,y)}{\partial t} = c\triangle u(t,x,y) = c\big(\frac{\partial^2 u(t,x,y)}{\partial x^2} + \frac{\partial^2 u(t,x,y)}{\partial y^2}\big), \quad t \geq 0, (x,y) \in \mathbb{R}^2 \tag{2.1}$$

with initial condition

$$u(0,x,y) = \phi(x,y). \tag{2.2}$$

We consider that $\phi(x,y)$ is defined on $[0,1]\times[0,1]$ and c is the diffusivity constatnt. This way of extending $\phi(x,y)$ is classical in image processing. In this manner it satisfies

$$\int_\Omega |\phi(X)|dX < +\infty. \tag{2.3}$$

That is $\phi(x,y) \in \mathbb{L}^1(\Omega)$, $X = (x,y)$.
Solving (2.1) is equivalent to carrying out a Gaussian linear filtering, which is an important part of signal processing and widely used. Let $\phi(x,y) \in \mathbb{L}^1(\Omega)$, $\Omega = [-1,1] \times [-1,1]$. Then the explicit solution of (2.1) is given by,

$$u(t,x,y) = \int_{\mathbb{R}^2} G_{\sqrt{2t}}(X-Y)\phi(Y)dY = (G_{\sqrt{2t}} * \phi)(X), \tag{2.4}$$

$$G_\sigma(X) = \frac{1}{2\pi\sigma^2} e^{-\frac{|X|^2}{2\sigma^2}}, \tag{2.5}$$

where, $G_\sigma(X)$ denotes the two dimensional Gaussian kernel. Convolution by a positive kernel is the basic operation in linear image filtering. It corresponds to low pass filtering. Equation (2.4) is the unique solution of (2.1) satisfying the following inequality:

$$Sup_{X\in\mathbb{R}^2}|u(t,x,y)| \leq c(t_1)|\phi(x,y)|_{\mathbb{L}^1(\Omega)}, \tag{2.6}$$

where $c(t_1)$ is a constant such that $t \in [t_1,\infty)$ and t_1 is a positive number.

If $\phi(x,y) \in \mathbb{L}^\infty$, then we have a maximum principle,

$$Inf_{X\in\mathbb{R}^2}\big(\phi(x,y)\big) \leq u(t,x,y) \leq Sup_{X\in\mathbb{R}^2}\big(\phi(x,y)\big). \tag{2.7}$$

It is well known that the equation (2.1) in $(0,T)\times\mathbb{R}^2$ with $u(0,x,y) = 0$ has infinitely many solutions and each nontrivial solution grows rapidly as $|X| \longrightarrow \infty$ to get a uniqueness result. It suffices to impose that u satisfies the growth estimate

$$|u(t,X)| \leq Ae^{\alpha|X|^2}, \tag{2.8}$$

for some constant A and $\alpha > 0$. For more details, see ([15] and [22], [27] and [32]).

3. Wavelet Transform

One of the important application of the wavelet transform in image processing is edge detection. While using linear diffusion equation we are left with edge that is the linear diffusion equations are not capable to capture the edges of the images during denoising process. In digital images, edges appear when there is an abrupt change in pixel intensities. So, this drawback can be handled by using wavelet denoising technique.

3.1. Wavelet Transform.

Definition 3.1. Wavelet is a small wave function(signal) with limited time duration and zero-mean in amplitude. It can also be called mother wavelet that satisfies:
(i) Total area under the wavelet is zero, i.e $\int_{-\infty}^{+\infty}\psi(t)dt = 0$,and
(ii) Total area of $|\psi(t)|^2$ is finite, i.e $\int_{-\infty}^{+\infty}|\psi(t)|^2dt < \infty$,
where ψ is the mother wavelet.
In other words a square integrable function ψ is called a wavelet, if it satisfies the admissibility condition,

$$\int_{-\infty}^{+\infty}\frac{|\hat{\psi}(\omega)|^2}{|\omega|}d\omega < \infty,$$

where, $\hat{\psi}$ is the Fourier transform of ψ which is given as follows ([4], [28], [29], [30]):

$$\hat{\psi}(\omega) = \int_{-\infty}^{+\infty}\psi(t)e^{-i\omega t}dt.$$

Definition 3.2. Wavelet transform of a function $f(t)$ is given by

$$W_{a,b}f = \int_{-\infty}^{+\infty} f(t)\frac{1}{\sqrt{|a|}}\psi^*(\frac{t-b}{a})dt, \tag{3.1}$$

where ψ^* is complex conjugate of mother wavelet ψ.

Definition 3.3. The inverse wavelet transform can be used to reconstruct the signal as

$$f(t) = \frac{1}{C}\int_{-\infty}^{+\infty}\int_{-\infty}^{+\infty} W_{a,b}\psi_{a,b}(t)db\frac{da}{a^2}, \tag{3.2}$$

where C is given by $C = \int_{-\infty}^{+\infty}\frac{|\psi(\omega)|^2}{|\omega|}$ and $\psi_{a,b}(t) = \psi(\frac{t-b}{a})$, see ([3], [6], [8], [17], [20], [21] and [24].

3.2. Discrete Wavelet Transform. The discrete wavelet transform is the heart of the signal processing which was proposed by Stephane Mallat [39] and [40] in 1989. The discrete form of a scaling function ϕ and wavelet functionψ can be written as $\{\phi_{j,k}(t) = 2^{j/2}\phi(2^j t-k) : k \in \mathbb{Z}\}$ and $\{\psi_{j,k}(t) = 2^{j/2}\psi(2^j t-k) : k \in \mathbb{Z}\}$, respectively since the set $\{\phi_{j,k}(t) : k \in \mathbb{Z}\}$ forms an orthonormal basis for the subspace $\{V_j : j \in \mathbb{Z}\}$, see the definition of multiresolution analysis ([8], [17], [20], [21] and [24]). Hence ϕ and ψ can be expressed as follows:

$$\phi(t) = 2^{1/2}\sum_{k\in\mathbb{Z}} h_k\phi(2t-k),$$
$$\psi(t) = 2^{1/2}\sum_{k\in\mathbb{Z}} g_k\psi(2t-k),$$

where $g_k = (-1)^{k+1}\overline{h_{1-k}}$.

Definition 3.4. Discrete wavelet transform of a function or signal $f[n]$ is given by

$$f[n] = \frac{1}{\sqrt{N}}\sum_{k\in\mathbb{Z}} h_k\phi_{j_0,k}[n] + \frac{1}{\sqrt{N}}\sum_{j=j_0}^{\infty}\sum_{k\in\mathbb{Z}} g_k\psi_{j,k}[n], \tag{3.3}$$

where, $f[n]$, $\phi_{j,k}$ and $\psi_{j,k}$ are defined on $[0,N-1]$, total N points and the coefficients h_k, g_k are low pass filters (approximation coefficients) and high pass filters (detailed coefficients), respectively, which can be calculated as follows ([31], [37], [41] and [42]):

$$h_k = \frac{1}{\sqrt{N}}\sum_{n\in\mathbb{Z}} f[n]\phi_{j_0,k}[n],$$
$$g_k = \frac{1}{\sqrt{N}}\sum_{n\in\mathbb{Z}} f[n]\psi_{j_0,k}[n], \quad j \geqslant j_0.$$

The decomposition of a signal by wavelet is given in Figure 1 and the reconstruction of the signal by wavelet has been shown in Figure 2. In Figure 1, *LoD* represents the low pass decomposition filter and *HiD* represents the high pass decomposition filter. In Figure 2, *LoR* represents the low pass reconstruction filter and *HiR* represents the high pass reconstruction filter. Further, $\uparrow 2$ and $\downarrow 2$ represent the up-sampling and down-sampling, respectively, see ([9], [19], [20], [24], [37], [39], [40], [41] and [42]).

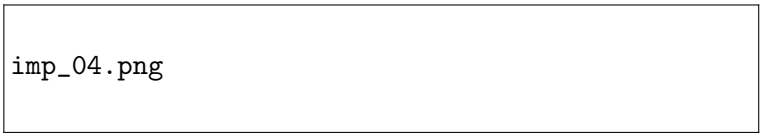

Figure 1. Discrete wavelet decomposition of signal.

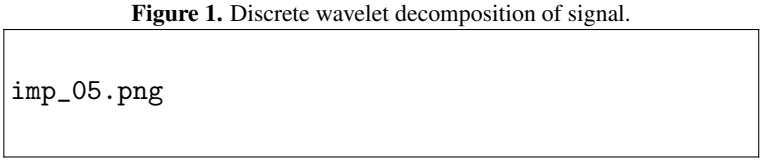

Figure 2. Discrete wavelet reconstruction of decomposed signal.

3.3. Two Dimensional Discrete Wavelet Transform. The two dimensional discrete wavelet transform of a discrete (digital) image $I_m = [I_{i,j}]_{1\le i\le M, 1\le j\le N}$, of size $M \times N$, where $I_{i,j}$ are real numbers given as:

$$\tilde{I_m} = W_M I_m W_N^T, \tag{3.4}$$

where, $W_M = \begin{pmatrix} H_{N/2} \\ G_{N/2} \end{pmatrix}$, $H_{N/2}$ and $G_{N/2}$ are high and low pass filter coefficients matrices.
The above transformation can be written as

$$\tilde{I_m} = W_M I_m W_N^T = \begin{pmatrix} H_{M/2} \\ G_{M/2} \end{pmatrix} I_m \begin{pmatrix} H_{N/2} \\ G_{N/2} \end{pmatrix}^T = \begin{pmatrix} H_{M/2} I_m \\ G_{M/2} I_m \end{pmatrix} \begin{pmatrix} H_{N/2}^T & G_{N/2}^T \end{pmatrix} \tag{3.5}$$

$$= \begin{pmatrix} H_{M/2} I_m H_{N/2}^T & H_{M/2} I_m G_{N/2}^T \\ G_{M/2}^T I_m H_{N/2}^T & G_{M/2} I_m G_{N/2}^T \end{pmatrix}$$

$$= \begin{pmatrix} \mathscr{A} & \mathscr{V} \\ \mathscr{H} & \mathscr{D} \end{pmatrix} = \begin{pmatrix} average & vertical\ difference \\ horizontal\ difference & diagonal\ difference \end{pmatrix} \tag{3.6}$$

where

$$\mathscr{A} = H_M I_m H_N^T, \quad \mathscr{V} = H_{M/2} I_m G_{N/2}^T, \quad \mathscr{H} = G_{M/2}^T I_m H_{N/2}^T, \quad and \quad \mathscr{D} = G_{M/2} I_m G_{N/2}^T.$$

Here $\mathscr{A}$ is averaged lower resolution version of the image I_m which is computed along row of I_m followed by computing average along columns, $\mathscr{H}$ is computed by trend (average) along row of image I_m followed by computation fluctuation along column, where as horizontal edges in an image fluctuation along column are able to detect these edges. This tends to emphasize the horizontal edges. $\mathscr{V}$ is similar to $\mathscr{H}$ roles of horizontal and vertical reverses. $\mathscr{V}$ is vertical fluctuation which is able to detect vertical edges of the image. $\mathscr{D}$ is diagonal fluctuation and emphasizes diagonal features created by both fluctuations along row and column. This fluctuation tends to erase vertical and horizontal edges ([9], [19] and [42]).
Now, let us suppose that, $\mathscr{A} = [a_{i,j}]$, $\mathscr{V} = [v_{i,j}]$, $\mathscr{H} = [h_{i,j}]$ and $\mathscr{D} = [d_{i,j}]$, $i = 1, 2, ..., \frac{M}{2}$; $j = 1, 2, ..., \frac{N}{2}$. In case of Haar wavelet the matrix W is given as follows:

$$W = \frac{1}{\sqrt{2}} \begin{pmatrix} 1 & 1 & 0 & 0 & 0 & ... & 0 & 0 \\ 0 & 0 & 1 & 1 & 0 & ... & 0 & 0 \\ . & . & . & . & . & . & . & . \\ . & . & . & . & . & . & . & . \\ 0 & 0 & 0 & 0 & 0 & . & 1 & 1 \\ 1 & -1 & 0 & 0 & 0 & ... & 0 & 0 \\ 0 & 0 & 1 & -1 & 0 & ... & 0 & 0 \\ . & . & . & . & . & . & . & . \\ . & . & . & . & . & . & . & . \\ 0 & 0 & 0 & 0 & 0 & . & 1 & -1 \end{pmatrix}, \tag{3.7}$$

The elements of the average, vertical, horizontal and diagonal matrices are given as follows:

$$\begin{aligned} a_{i,j} &= \frac{I_{m_{2i-1,2j-1}} + I_{m_{2i-1,2j}} + I_{m_{2i,2j-1}} + I_{m_{2i,2j}}}{2}, \\ v_{i,j} &= \frac{(I_{m_{2i-1,2j-1}} + I_{m_{2i,2j-1}}) - (I_{m_{2i-1,2j}} + I_{m_{2i,2j}})}{2}, \\ h_{i,j} &= \frac{(I_{m_{2i-1,2j-1}} + I_{m_{2i-1,2j}}) - (I_{m_{2i,2j-1}} + I_{m_{2i,2j}})}{2}, \\ d_{i,j} &= \frac{(I_{m_{2i-1,2j-1}} + I_{m_{2i,2j}}) - (I_{m_{2i-1,2j}} + I_{m_{2i,2j-1}})}{2}. \end{aligned}$$

Since the matrices W_N and W_M are orthogonal, the inverse discrete wavelet transform of the image I_m can be calculated as follows:

$$\begin{aligned} \tilde{I_m} &= W_M I_m W_N^T, \\ W_M^T \tilde{I_m} &= I_m W_N^T, \\ W_M^T \tilde{I_m} W_N &= I_m, \\ I_m &= W_M^T \tilde{I_m} W_N. \end{aligned}$$

The wavelet decomposition of an image is given in Figure 3 and the reconstruction of the image by wavelet has been shown in Figure 4. In Figure 3, *LoD* represents the low pass decomposition filter, $\downarrow 2$ represents the down-sampling and *HiD* represents the high pass decomposition filter. In Figure 4, *LoR* represents the low pass reconstruction filter, $\uparrow 2$ represent the up-sampling and *HiR* represents the high pass reconstruction filter. Further, j denotes the level of decomposition , a^j is average of the image at j^{th} level, d_h^{j+1}, d_v^{j+1}, d_d^{j+1} represents the horizontal, vertical and diagonal differences at j^{th} level.

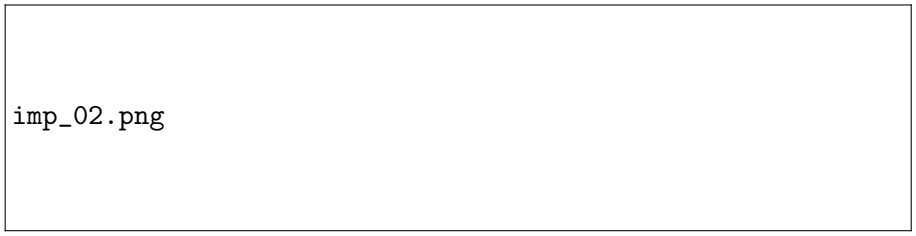

Figure 3. Basic step for the decomposition in wavelets for images.

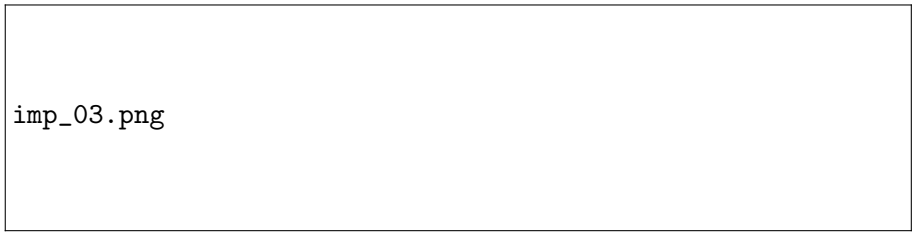

Figure 4. Basic step for wavelet reconstruction for decomposed images.

DWT allows for analyzing the noise level separately at each wavelet scale and adapted the denoising algorithm accordingly. For denoising, a wavelet should be able to capture the transient spikes of the original image then select those detail coefficients which are larger than the characteristics of the amplitude of noise and discard others, the selection is based on thresholding of the detail coefficients. The basic concept of image denoising by wavelet is based on choosing a thresholding. A threshold value T is chosen for which all transform values are linear in magnitude then T set equal to zero. By performing inverse wavelet transform on the thresholded transform, an estimation of the original signal is estimated. There are two types of thresholdings occur namely Hard and Soft. Once the thresholdings rule have been selected only the essential ingredient remains to be found the noise level that is the estimation of noise level. Mainly two families are there; first one is Donoho and Johnstone methods which contains Square2log, SURE, HeurSure and Minimax. SURE and HeurSure are level dependent threshold while Square2log and and Minimax are global threshold. The second family is Birge-Massart which is level dependent and penalized globally, see ([10]-[13], [18], [19], [23] and [37]).

4. Proposed Model

Let us assume that $u_0(x,y)$ is the noisy image and $u(x,y)$ is the original image or clear image without noise and $n(x,y)$ is the additive white Gaussian noise such that

$$u_0(x,y) = u(x,y) + n(x,y). \tag{4.1}$$

Now, let us suppose that $u_0(x,y)$ is an initial solution of the linear diffusion equation (2.1) such that

$$u(0,x,y) = \phi(x,y) = u_0(x,y) = u(x,y) + n(x,y). \tag{4.2}$$

To solve the diffusion equation (2.1), we use forward finite difference formulae ([15], [16], [25] and [26]), as follows:

$$u_{xx} = \frac{u^n_{i+1,j} - 2u^n_{i,j} + u^n_{i-1,j}}{\Delta x^2}, \tag{4.3}$$

$$u_{yy} = \frac{u^n_{i,j+1} - 2u^n_{i,j} + u^n_{i,j-1}}{\Delta y^2}, \tag{4.4}$$

$$u_t = \frac{u^{n+1}_{i,j} - u^n_{i,j}}{\Delta t}. \tag{4.5}$$

Now, using equations (4.3), (4.4) and (4.5) in equation (2.1), we get

$$\frac{u_{i,j}^{n+1}-u_{i,j}^{n}}{\Delta t}=c\left(\frac{u_{i+1,j}^{n}-2u_{i,j}^{n}+u_{i-1,j}^{n}}{\Delta x^{2}}+\frac{u_{i,j+1}^{n}-2u_{i,j}^{n}+u_{i,j-1}^{n}}{\Delta y^{2}}\right). \tag{4.6}$$

By taking $\Delta x=\Delta y$ and solving, we get

$$u_{i,j}^{n+1}=u_{i,j}^{n}+\frac{c\Delta t}{\Delta x^{2}}\left(u_{i+1,j}^{n}-2u_{i,j}^{n}+u_{i-1,j}^{n}+u_{i,j+1}^{n}-2u_{i,j}^{n}+u_{i,j-1}^{n}\right). \tag{4.7}$$

This system is stable if $\frac{\Delta t}{\Delta x^{2}}\leq 0.5$ (see the proof in [15], [16], [25] and [26]). Further, the above system (4.7) is solved with the help of equation (4.1) and we assume that the obtained solution is $I(x,y)$. Now, we apply the discrete wavelet transform on $I(x,y)$ as we did in equation (3.4) and get $\tilde{I}(x,y)$, that is

$$\tilde{I}(x,y)=W_{M}I(x,y)W_{N}^{T}. \tag{4.8}$$

On solving we get

$$\tilde{I}(x,y)=\begin{pmatrix}\mathscr{A} & \mathscr{V}\\ \mathscr{H} & \mathscr{D}\end{pmatrix}. \tag{4.9}$$

Now, we shall apply the thresholding technique on $\tilde{I}(x,y)$ (in our case we use soft thresholding). After threshold we apply inverse discrete wavelet transform on $\tilde{I}(x,y)$ as we did in equation (3.9) and then, we obtain

$$I(x,y)=W_{M}^{T}\tilde{I}(x,y)W_{N}, \tag{4.10}$$

which is the required denoised image.

For numerical computation and comparison with other existing methods we computed the mean square error and peak signal to noise ratio by following formulae:

$$MSE=\frac{1}{MN}\sum_{i=1}^{M}\sum_{j=1}^{N}\left(u(x,y)-I(x,y)\right)^{2}, \tag{4.11}$$

$$PSNR=10\frac{\log\left(\frac{MN}{MSE}\right)}{\log 10}. \tag{4.12}$$

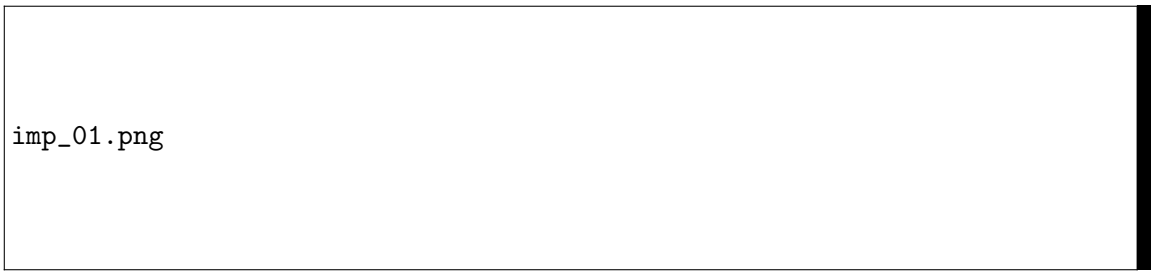

Figure 5. Flowchart of the algorithm for the proposed model.

Algorithm Input

Step 1: Load a clean Image $I(i,j)$,
Step 2: Generate random white Gaussian noise and add into the Image $I(i,j)$ and obtain

noisy image $\tilde{I}(i,j)$, i.e., $\tilde{I}(i,j) = I(i,j) + w(i,j)$,
Step 3: Apply the diffusion equation model by considering noisy image $\tilde{I}(i,j)$ as initial condition and obtain the solution of diffusion equation by using finite difference method, which is a smooth image,
Step 4: Apply the discrete wavelet transform on the image which is obtained as a solution of diffusion equation to decompose the image up-to appropriate level,
Step 5: Apply the threshold technique for thresholding,
Step 6: Reconstruct the clean image by computing inverse discrete wavelet transform,
Step 7: Compute the peak signal to noise ratio,
Output: Obtained denoised Image.

5. Simulations and Results

In this section, we have given some examples to evaluate and validate the performance of proposed technique. We took gray scale image contaminated with additive white Gaussian noise with zero mean and σ^2 variance (we added standard noise). In this experiment, we use Haar, Daubechies, Coiflets, Symlets, Franklin and Biorthogonal wavelets to denoise the noisy images. The values of peak signal to noise ratio (PSNR) are tabulated in the tables and figures of original, noisy and denoised images are given. We compared PSNR values obtained by proposed method with the wavelet method, diffusion equation method and method proposed by Kumar et al [38].

Example 1. In this example, we took the test image of Lena and then we added the standard random white gaussian noise. Further, we applied proposed technique to denoise the noisy image of Lena and calculated the PSNR values, which are tabulated in the tables 1.1 and 1.2, as well as, the original image 1(a), noisy image 1(b) and the denoised image 1(c) are represented. On applying diffusion equation model we obtained PSNR value 26.03 and on using wavelet denoising approach we obtained PSNR value 23.62. While using proposed method we obtained maximum PSNR value upto 31.5454, which is far better than other methods as well as method proposed by Kumar et al [38].

Table 1.1. Calculated PSNR values of denoised Lena image obtained by proposed model and corresponding wavelets for example 1.

Wavelet	PSNR	Wavelet	PSNR	Wavelet	PSNR	Wavelet	PSNR
Sym4L1	31.5276	Sym4L2	31.5430	Sym4L3	31.5454	Bi-orth. 2.2	31.4888
Daub.5	26.8263	Coif1	26.8386	Coif4	26.7673	Fra.	26.8379

Table 1.2. Calculated PSNR values of by different methods for example 1.

Noisy Image	[38]	Wavelet	Diff. eqn	Our method
18.7073	26.8263	23.62	26.03	31.5454

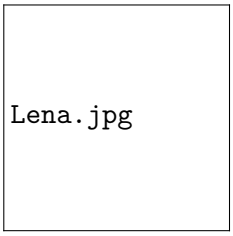

1(a). Original Lena image

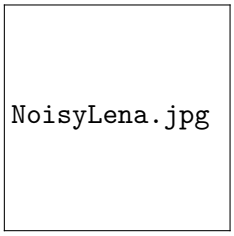

1(b). Noisy Lena image

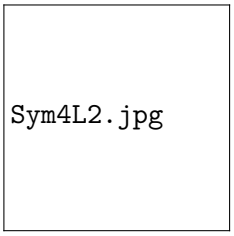

1(c). Denoised by our method

Example 2. In this example, we took the test image of Moon surface and then we added the random white Gaussian noise. Further, we applied proposed technique to denoise the noisy image of Moon surface and calculated the PSNR values, which are tabulated in the tables 2.1 and 2.2, as well as, the original image 2(a), noisy image 2(b) and the denoised image 2(c) are represented. On applying diffusion equation model we obtained PSNR value 28.18 and on using wavelet denoising approach we obtained PSNR value 21.08. While on using proposed method we obtained maximum PSNR value upto 28.2996, which is far better than other methods.

Table 2.1 Calculated PSNR values of denoised Moon image obtained by proposed model and corresponding wavelets for example 2.

Wavelet	PSNR	Wavelet	PSNR	Wavelet	PSNR	Wavelet	PSNR
HaarL2	28.2190	Sym3	28.2996	Sym4	28.2524	Sym5	28.2781
Daub.5	28.2402	Coif1	28.2411	Coif5	28.2554	Fra.	28.2586

Table 2.2. Calculated PSNR values of by different methods for example 2.

Noisy Image	Wavelet	Diff. eqn	Our method
19.99	21.08	28.18	28.2996

2(a). Original Moon Surface

2(b). Noisy Moon Surface

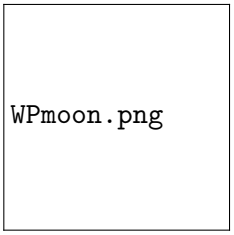

2(c.) Denoised by our method

Example 3. In this example, we took the test image of clock and then we added the random white Gaussian noise. Further, we applied proposed technique to denoise the noisy image of clock and calculated the PSNR values, which are tabulated in the tables 3.1 and 3.2, as well as, the original image 3(a), noisy image 3(b) and the denoised image 3(c) are represented. On applying diffusion equation model we obtained PSNR value 26.0323 and on using only wavelet denoising approach we obtained PSNR value 21.7410. While

on using proposed method we obtained maximum PSNR value upto 26.9786, which is far better than other methods.

Table 3.1. Calculated PSNR values of denoised clock image obtained by proposed model and corresponding wavelets for example 3.

Wavelet	PSNR	Wavelet	PSNR	Wavelet	PSNR	Wavelet	PSNR
Haar	26.9786	Daub. 7	26.8998	coif. 3	26.9362	Sym.5	26.9752
Daub. 3	26.9301	Daub. 9	26.8326	coif. 5	26.9104	Bi-orth. 2.2	26.8743
Daub. 5	26.9265	Daub. 45	26.7551	Sym.4	26.9203	Bi-orth. 3.5	26.7663

Table 3.2. Calculated PSNR values by different methods for example 3.

Noisy Image	Wavelet	Diff. eqn	Our method
20.6049	21.7410	26.023	26.9786

3(a). Original Clock image

3(b). Noisy Clock image

3(c). Denoised by our method

Example 4. In this example, we took the test image of Airplane and then we added the random white Gaussian noise. Further, we applied proposed technique to denoise the noisy image of Airplane and calculated the PSNR values, which are tabulated in the tables 4.1 and 4.2, as well as, the original image 4(a), noisy image 4(b) and the denoised image 4(c) are represented. On applying diffusion equation model we obtained PSNR value 27.5971 and on using wavelet denoising approach we obtained PSNR value 21.53. While on using proposed method we obtained maximum PSNR value upto 28.0610, which is far better than other methods.

Table 4.1 Calculated PSNR values of denoised Airplane image obtained by proposed model and corresponding wavelets for example 4.

Wavelet	PSNR	Wavelet	PSNR	Wavelet	PSNR	Wavelet	PSNR
HaarL2	27.9290	Sym4L1	27.6921	Sym4L2	27.8631	Sym4L3	27.9727
Daub.5	28.0251	Coif1	28.0610	Coif4	27.9879	Fra.	28.0497

Table 4.2. Calculated PSNR values by different methods for example 4.

Noisy Image	Wavelet	Diff. eqn	Our method
19.3695	21.53	27.5971	28.0610

4(a). Original Airplane image

4(b.) Noisy Airplane image

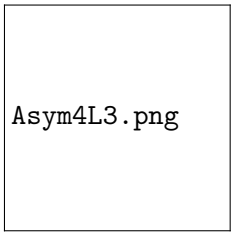

4(c). Denoised by our method

Conclusion

We have applied the diffusion equation and wavelet based model on noisy images which are contaminated with standard noise to denoise the noisy image. We obtained the PSNR values which are tabulated in the tables and the corresponding figures are also given. To show the performance of the proposed method we denoise four test images and compared the calculated PSNR values with existing methods. In the proposed method, we obtained the PSNR value upto 31 for Lena image, while on using diffusion equation model we get the PSNR 26.03. Further, on using wavelet denoising method we get the PSNR value 23.62 and in the model proposed by Kumar [38] PSNR value is 25.34. This shows the superiority of our method. In this paper we use Haar, Daubechies, Symlet, Coiflet, Franklin and Biorthogonal wavelets and decomposed the images upto appropriate level of decomposition and soft thresholding for denoising.

Acknowledgment. The authors are thankful to the reviewers for their helpful comments which substantially improved the quality of the manuscript.

References

1. A. Beck and M. Teboulle, A fast iterative shrinkage-thresholding algorithm for linear inverse problems, SIAM J. Imag. Sci., 2(1), 183-202, (2009).
2. A. Pizurica and W. Philips, Estimating the probability of the presence of a signal of interest in multiresolution signal and multiband image denoising, IEEE Trans. Ima. Proc., 15(3), 645-665, (2006).
3. A. Raza and A. Khan, Haar wavelet series solution for solving neutral delay differential equations, J. King Saud University-Science, 31, 1070-1076, (2019).
4. A. Raza, A. Khan, P. Sharma and K. Ahmad, Solution of singularly perturbed differential difference equations and convection delayed dominated diffusion equations using Haar wavelet, Math. Sci., 15, 2, 123-136, (2021).
5. C. Liu, R. Szelisci and S. B. Kang, Automatic estimation and removal of noise from a single image, IEEE Trans. Pattern Anal. Mach. Intell., 30(2), 299-314, (2008).
6. C. K. Chui, An Introduction to Wavelets. Academic Press, San Diego, 49-74 (1992).
7. C. Schnorr, Unique reconstruction of piecewise smooth images by minimizing strictly convex non-quadratic functionals. J. Math. Imag. Vis., 4, 189-198, (1998).
8. D. F. Walnut, An Introduction to Wavelet Analysis, Birkhauser Boston, (2002).
9. D. K. Ruch and P. J. Van Fleet, Wavelet theory an elementary approach with applications, John Wiley and Sons, Inc., Hoboken, New Jersey (2009).

10. D. L. Donoho, Wavelet shrinkage and W. V. D., A 10-minute tour, in Int. Conf. Wavelets and Applications, Stanford University, Toulouse, France (1992).
11. D. L. Donoho, De-noising by soft thresholding, IEEE Trans. Inf. Theory, 41(3) 613-627, (1995).
12. D. L. Donoho and I. M. Johnstone, Ideal spatial adaptation via wavelet shrinkage,Biometrika, 81(3), 425-455, (1994).
13. D. L. Donoho and I. M. Johnstone, Adapting to unknown smoothness via wavelet shrinkage, J. Amer. Stat. Asso., 90, 432 , 1200-1224, (1995).
14. F. Yan, L. Cheng and S. Peng, A new interscale and intrascale orthonormal wavelet thresholding for SURE-based image denoising, IEEE Trans. Sig. Pro. Lett., 15, 139-142, (2008).
15. G. Aubert and P. Kornprobst, Mathematical Problems in Image Processing Partial Differential Equations and the Calculus of Variations (Second Edition), Springer (USA), 2006.
16. G. D. Smith, Numerical Solution of Partial Differential Equations (3rd edn) (Oxford University Press), (1985).
17. I. Daubechies, Orthonormal bases of compactly supported wavelets, Comm. Pure Appl. Math., 41, 909-996, (1988).
18. I. M. Johnstone and B. W. Silverman, Wavelet threshold estimator for data with correlated noise, J. Roy. Statist. Sco. B., 59, 319-351, (1997).
19. J. S. Walker, A Primer on Wavelets and their Scientific Applications, 2nd Edition, Chapman and Hall/CRC, Boca Raton, London, New York, USA, (2008).
20. K. Ahmad and Abdullah, Wavelet Packets and Their Statistical Applications, Springer Singapore, (2018).
21. K. Ahmad and F.A. Shah, Introduction to Wavelets with Applications, Real World Education Publishers, New Delhi, (2013).
22. K. Bredies and D. Lorenz, Mathematical Image Processing, Applied and Numerical Harmonic Analysis, Springer Nature Switzerland AG, (2018).
23. L. Birge, P. Massart, From model selection to adaptive estimation, in D. Pollard (ed), Festchrift for L. Le Cam, Springer, 55-88, (1997).
24. L. Debnath, and F. A. Shah, Wavelet Transform and their Applications, Springer New York, Birkhauser, 337-440, (2015).
25. L. Lapidus and G. F. Pinder, Numerical solution of partial differential equations in science and engineering. SIAM Rev, 25(4), 581-582, (1983).
26. M. K. Jain, Numerical Solution of Differential Equations (2nd edn) (New Delhi: Wiley Eastern), (1984).
27. M. Welk, Theis D, Brox T and Weickert J, PDE-based deconvolution with fordward-backward diffusivities and diffusion tensors. In: Scale space, LNCS, pp 585-597. Springer, Berlin,(2005).
28. Mo. Faheem, A. Khan and A. Raza, Solution of the third order Emden Fowler type equation using wavelet method, Eng. comp., Emrald, (2021).
29. Mo. Faheem, A. Raza and A. Khan, Collocation method based on Gegenbauer and Bernoulli wavelet for solving neutral delay differential equations, Math. Comp. Sim., Elsevier, 180, 72-92, (2021).
30. Mo. Faheem, A. Raza and A. Khan, Wavelet collocation methods for solving neutral delay differential equations, Int. J. Non. Sci. Num. Sim., (2021).
31. O. Christensen, K. L. Christensen, Approximation Theory From Taylor Polynomials to Wavelets, Birkhauser Boston Springer-Verlag New York, (2004).
32. O. Scherzer, Denoising with higher order derivatives of bounded variation and an application to parameter estimation. Computing, 60(1),127, (1994).
33. P. Sharma, K. Khan and K. Ahmad, Image denoising using local contrast and adaptive mean in wavelet transform domain. Int. J. Wave. Multi. Inf. Pro., 12(6), (2014). doi:10.1142/S0219691314500386
34. Q. Chang and I. L. Chern, Acceleration methods for total variationbased image denoising. SIAM J. Sci. Comp., 25(3),982-994,(2003).
35. S. G. Chang, B. Yu and M. Vetterli, Adaptive wavelet thresholding for image denoising and compression, IEEE Trans. Image Process., 9(9), 1135–1151, (2000).
36. T. F. Chan , G. H. Golub, P. Mulet, A nonlinear primal-dual method for total variation based image restoration. SIAM J. Sci. Comp. 20(6), 1964-1977, (1999).
37. R. R. Coifman, Y. Meyer and M. V. Wickerhauser, Wavelet analysis and signal processing, in Wavelets and Their Applications (M.B. Ruskai et al., Eds.), Jones and Bartlett Publishers, Boston, 153-178, (1992).
38. S. Kumar, M. Sarfaraz and M. K. Ahmad, Denoising method based on wavelet coefficients via diffusion equation, Iran J. Sci. Tech. Tran. Sci., (2017). DOI 10.1007/s40995-017-0228-7.

39. S. G. Mallat, A theory for multiresolution signal decomposition:the wavelet representation. IEEE Trans. Pattern Anal. Mach. Intell., 11(7), 674-693, (1989).
40. S. G. Mallat, Multiresolution approximations and wavelet orthonormal bases of $L^2(R)$; Trans. Amer. Math. Soc., 315 , 69-87, (1989).
41. W. Hardle, G. Kerkyacharian, D. Picard and A. Tsybakov, Wavelets, App. Stat. App., Springer, (1998).
42. Y. Nievergelt, Wavelets made easy, Springer, 978-1-4612-0573-9, (1999).

[1] Department of Mathematics, Jamia Millia Islamia, New Delhi-110025, India.
Email address: akmalrazataqvi@gmail.com

[1] Department of Mathematics, Jamia Millia Islamia, New Delhi-110025, India.
Email address: akhan2@jmi.ac.in

[2] Department of Mathematics ,Al-Falah University,Faridabad(Haryana) India.
Email address: kahmad49@gmail.com